Hindawi
Advances in Civil Engineering
Volume 2022, Article ID 5995103, 12 pages
https://doi.org/10.1155/2022/5995103

Research Article

A Study on Using Glass Fiber-Reinforced Polymer Composites for Shear and Flexural Enhancement of Reinforced Concrete Beams

Hibretu Kaske Kassa,[1] **Getinet Melesse**,[2] **and Gashahun Yabasa**[2]

[1]*Department of Civil Engineering, Debre Tabor University, South Gondar, Ethiopia*
[2]*School of Civil Engineering, Institute of Technology, Arbaminch University, Arbaminch, Ethiopia*

Correspondence should be addressed to Hibretu Kaske Kassa; hibretuk2015@gmail.com

Received 23 December 2021; Revised 3 May 2022; Accepted 19 May 2022; Published 22 June 2022

Academic Editor: Luigi Fenu

In the concrete construction sector, issues such as tensile strength of structural elements, brittle mode of failure, rapid crack propagation, and increased overload are common. The experimental evaluation of the flexural strengths of glass fiber-reinforced polymers with various percent of glass fiber content is the focus of this study. Fiber-reinforced polymer is the focus of numerous studies right now all over the world. Experimental investigations done on the behavior of the concrete strengthened using discontinuous chopped glass fiber were carried out with C-25 concrete mix and 50 mm of glass fiber at various percentages (0.25%, 0.50%, 0.75%) of addition by the total weight of concrete. Experimental data on load for flexural tests have been carried out. Strength variations and failure modes of each specimen have been obtained. According to ASTM standards, at 7, 21, and 28 days after casting, all beams, such as control and fiber-reinforced concrete beams, are tested by third point loading. The results of the flexural test indicated that the presence of glass fiber tends to increase the flexural strength of concrete at higher fiber content, and the bending test results indicated that the modulus of rupture of concrete in set I increases by 2.5% at 0.25% glass fiber, 11.3% at 0.50% glass fiber, 13.2% at 0.75% glass fiber at the end of 7 days, 1.19% at 0.25% glass fiber, 2.38% at 0.50% glass fiber and 9.94% at 0.75% glass fiber at the end of 21 days, 0.54% at 0.25% glass fiber, 1.89 at 0.50% glass fiber, and 2.45% at 0.75% glass fiber at the end of 28 days. Thus, ductility improves after concrete cracking, with 2.19% at 0.25% glass fiber, 10.19% at 0.50% glass fiber, and 13.60% at 0.75% glass fiber at the end of 28 days. As a result, the flexural strength of the content improves as well.

1. Introduction

Due to its remarkable mechanical properties while being light, low cost, and incredibly flexible, a composite material is one of the most popular engineering materials. Composites are constructed, composed of a matrix that surrounds the reinforcement, and gives the strength and durability needed in a certain field. FRP composite materials have been effectively used in the construction of new structures as well as the restoration of existing structures, and they hold a lot of promise for the construction industry's future. Strengthening of reinforced concrete and prestressed concrete structural elements may be required due to increased service loads, changes in usage patterns, structural degradation of concrete, or design or construction defects.

Tests of eleven SFRC beams subjected to reversal cyclic loading and numerical analysis using 3D finite element (FE) modeling are used to study the hysteretic response of slender and deep steel fiber-reinforced concrete (SFRC) beams reinforced with steel reinforcement. The experimental program includes flexural and shear-critical SFRC beams with various steel reinforcing bar ratios (0.55 percent and 1.0 percent), closed stirrups (from 0 to 0.5 percent), and fiber content ranging from 0.5 to 3% per volume. For the post-cracking behavior of SFRC under tension, a smeared crack model is given, which exploits the fracture characteristics of the composite material using stress vs. crack width curves with tension softening. To support the experimental research and verify the proposed model, axial tension tests on prismatic SFRC specimens were used. When comparing

computational and experimental findings, the proposed model is found to be efficient and accurate in capturing key characteristics of the response, such as the SFRC tension softening effect, the load versus deformation cyclic envelope, and the role of fibers on overall hysteretic performance [1].

In reference [2], the properties of composites made from chopped strand mat and woven roving E-glass fiber were investigated. Chopped strand mat composites outperformed woven roving E-glass fiber composites in terms of mechanical characteristics. [3] Chopped glass fiber-reinforced polyester composites subjected to flexural and compression stresses were evaluated for in-planer shear strength and failure behavior. The results of the experiments were compared to analytical predictions such as maximum stress and strain. Concrete's compressive and tensile strengths were also improved. [4] Casting and testing of a $100\,\text{mm} \times 100\,\text{mm} \times 500\,\text{mm}$ RC beam with a concrete mix design for C-30 grade concrete are part of the experimental program. The volume of chopped strands of basalt fiber was added at $1\,\text{kg/m}^3$, $2\,\text{kg/m}^3$, and $4\,\text{kg/m}^3$ for each mix of concrete specimens. The flexural strength of fiber concrete increased by 54% when the fiber content was increased to $4\,\text{kg/m}^3$. It was found from the failure pattern of the specimens that the formation of cracks was greater in the case of concrete without fibers than in the case of fiber-reinforced concrete. As evidenced by this, the presence of basalt fibers in the concrete functions as a crack arrestor. The inclusion of fibers increased the ductility properties. In comparison to the brittle failure of plain concrete, fiber concrete failure was gradual. The author concluded from the findings that the percentage increase in the strength of fiber-reinforced concrete increases with the concrete's age.

Reference [5] studied that 1.5wt% vinyl ester (VE)/organoclay and 2wt% epoxy (EP)/organoclay nanocomposites were prepared by an in situ polymerization method. To investigate the effects of a nanocomposite matrix on the durability of GFRP composites, GFRP composites were fabricated with 1.5wt percent VE/clay and 2.0wt percent EP/clay nanocomposites. Tensile properties of GFRP specimens aged in water and alkaline solution at 60°C were monitored to characterize the durability of the two types of GFRP composites, and SEM was used to investigate the fracture behaviors of aged GFRP composites under tension. The findings reveal that the tensile characteristics of both types of GFRP composites with and without clay deteriorate significantly over time. However, when GFRP composites with nano-clay are compared with those without nano-clay, the degradation rate is lower, and the EP/GFRP modification improves the durability more effectively.

Experimentally, the behavior of reinforced concrete beams with steel fibers as mass reinforcement under torsion is explored. Steel fibers with a length-to-diameter ratio of 37.5 are employed. The experimental program includes plain concrete beams (control specimens), specimens with longitudinal reinforcing bars, and specimens with bars and stirrups and includes 35 beams with rectangular, L-shaped, and T-shaped cross-sections with various configurations of conventional and fiber steel reinforcement. Steel fiber volume fractions of 0%, 1%, and 3% are used to investigate all cases. In addition, the test findings revealed that fiber concrete beams outperformed nonfiber control beams in terms of overall torsional performance. Steel fibers were required for the tested beams that lacked or had insufficient conventional steel reinforcing. Fibers prevented sudden brittle failure of rectangular and nonrectangular beams, and they proved to be sufficient in some cases to give increased torsional moment capacities, even when stirrups were completely replaced with steel fibers [6].

In Reference [7], the impact strengths of epoxy and glass fiber composites in three different forms were compared, namely unidirectional, plain weave, and chopped strand mat. When composites with chopped strand mat were submitted to a single and repeated high velocity impact test, they found that they were more resistant to damage extension ([8, 9]). The mechanical properties of chopped strand E-glass and empty fruit bunch palm reinforced polylactide acid composites were examined. Solution casting, pillarization, and heat compression were used to make the composites. A constant fiber volume fraction of 20% was employed with varying ratios of chopped strand E-glass and empty fruit bunch palm fibers. Chopped strand E-glass fibers were used in composites to improve their strength and performance. The ability of fiber-reinforced composites is to improve the strength and stiffness of reinforced concrete flexural components. [10] Fiber-reinforced polymer composites are increasingly being investigated as an upgrade to and replacement for infrastructure components or systems composed of traditional construction materials such as concrete and steel. In an experimental setting, the effect of steel fibers on the response of RC beams subjected to reversal loading via a four-point bending method was investigated ([11, 12]). Three slender beams, each 2.5 m long with a rectangular cross section, were constructed and tested (two with steel fiber-reinforced concrete and one with plain-reinforced concrete). Steel fiber-reinforced concrete (SFRC) beams were reinforced with hook-ended steel fibers with a length-to-diameter ratio of 44 and two distinct volumetric fractions (1 percent and 3 percent). The damage indices, cracking performance, and failure of the tested beams were all given and addressed, as well as the hysteretic response based on energy dissipation capacities (also in terms of equivalent viscous damping). In comparison to the RC beam, test results showed that the SFRC beam had a better overall hysteretic response, higher absorbed energy capacities, superior cracking patterns, and a change in failure character from concrete crushing to ductile flexural failure. The nonfibrous reference specimen failed brittle after shear diagonal cracking, but the SFRC beam containing 1% steel fibers failed with sufficient ductility after concrete spalling. The SFRC beam with 3% steel fibers had a better cycle response, exhibiting pronounced flexural behavior with substantial ductility thanks to the fibers' capacity to transfer produced tensile stresses across fracture surfaces, preventing inclined shear cracks and concrete spalling.

In reference [13], the force transmission between the fiber and the matrix through an interfacial layer surrounding the fiber determines the pullout behavior. There are three different pullout load-bearing mechanisms to consider. The

first presupposes a complete link between matrix and fiber and is used to describe the elastic stage when there is no genuine "slip". The second is a transitional mechanism, which characterized the behavior as de bonding began, and the third is a frictional dynamic pullout mechanism based on matrix hydration shrinkage and a fibre-matrix misfit consideration. Behavioral features of the fibers and matrices were developed using experimental data and based on the analytical model. Pullout tests on hooked fibers have revealed that the superimposition of the hook's mechanical component with the bond frictional component derived from a straight fiber pullout can explain the hooked fibers' pullout behavior.

Reference [14] conducted a detailed parameter study based on five input variables, including the applied temperature, number of flange bolts, number of web bolts, length of the beam, and applied static loads, and performed nonlinear finite element simulations to predict the performance of a column-tree moment connection (CTMC) under fire and static loads. The first variable can be modified at seven different levels, while the remaining variables can be changed at three different levels. For the parameter study, 9 samples were designed using the Taguchi technique for variables 2–5 and their levels, with each sample being subjected to 7 different temperatures and giving 63 outputs. For the training and testing of different surrogate models, the corresponding variables for each output are imported. Multiple linear regression (MLR), multiple Ln equation regression (MLnER), an adaptive network-based fuzzy inference system (ANFIS), and gene expression programming are examples of surrogate models (GEP). The remaining samples were used for testing, while 44 samples were used for training. GEP beats MLR, MLnER, and ANFIS, according to our findings. The results show that the CTMC's rotation and deflection are temperature dependent. Furthermore, as the length of the beam is reduced, the fire resistance of the building increases; hence, a shorter beam can improve the building's fire resistance. At temperatures above 400°C, the number of flanges and web bolts has a minor impact on the rotation and displacement of the CTMCs. [15] Using nonlinear finite element analysis and surrogate models, the author's evaluated the resistance of reinforced concrete panels (RCPs) to explosive loads. To forecast the maximum deflection of RCPs, the gene expression programming model (GEP), multiple linear regression (MLR), multiple Ln equation regression (MLnER), and their combinations are utilized. Maximum positive and negative mistakes, mean absolute percentage error (MAPE), and statistical metrics such as coefficient of determination and root mean square error are all examples of maximum positive and negative errors (RMSE). The models' performances are evaluated and compared using normalized square error (NMSE) and fractional bias. We also show the distribution of percentage errors, suggesting that MLnER is the best model for forecasting the maximum deflection of RCPs under blast loading. The primary aim of this study is to understand the behavior of flexural enhancement of reinforced concrete beams utilizing GFRP composites in order to improve the RC beam's load-carrying capacity.

2. Material and Methods

2.1. Materials. The sample for a test was prepared by using the following materials. Ordinary portland cement that meets the prerequisite of Ethiopian national standard EN1177-1:2005 with a specific gravity of 3.15 is used. The fine aggregates used for experimental work are obtained from bed of river, and the aggregates are washed and dried. Before stepping on to other works, the specific gravity is determined and found as 2.62. The coarse aggregates used are nonreactive and as per the requirements to produce a good and durable concrete. The coarse aggregates are of two different grading and as such a definite mix proportion is used to obtain the desire grading for coarse aggregates. The maximum size is 20 mm and minimum 14.7 mm for concrete mix with the specific gravity is determined and found as 2.72. Ordinary tap water that is safe and potable for drinking and washing is used for producing the concrete. All deformed bar current strength is checked at the laboratory. Deformed bar's diameter of 10 mm is used in the tension and compression zone of concrete beam. The longitudinal reinforcing bars used for this experiment are high-yield strength of size 10 mm diameter and deformed bar diameter of 6 mm stirrups are used. The properties of the reinforcement steel are obtained from a tensile strength test in the laboratory. The averaged ultimate and yield tensile strengths are 632.38 MPa and 545.37 MPa, respectively.

Chopped strand mat (CSM) in this study is fine strand reinforcement material made from E-glass fibers. It is an excellent reinforcement material for translucent roofing panel and chemical storage tanks, FRP pipelines, boat hulls and decks, truck body panels, and other similar items are available. Glass fiber in Figure 1 known as fiberglass CSM-450 (TAISHAN) made in China. It is a lightweight, incredibly strong, and durable material. The most common synthetic fiber is glass fiber, which is chemically inert, hydrophobic, and lightweight. They are produced as continuous cylindrical monofilaments that can be chopped to lengths 50 mm, diameter 0.5 mm, and specific gravity 2.68. By far, the most common type of fiber found in composites is e-glass. These types have good combinations of chemical resistance, mechanical, and insulating properties. Furthermore, E-glass offers the more attractive economics. E-glass fibers are usually exist in three principal types including continue glass fiber, chopped glass fiber, and unidirectional glass fiber. The type of E-glass fiber which is used in this study is chopped E-glass type.

2.2. Mix of Concrete. The concrete mix and the quantity of materials used for 1 m^3 of concrete with a nominal maximum size of aggregate of 20 mm and high workability are given as follows: to find out the quantities of ingredients, the mix proportions for cement, sand, and coarse aggregates according to the standard mix for ordinary structural concrete per 50 kg of cement are 1 : 1.72 : 2.58, respectively. Table 1 shows how to prepare the mix design to conduct the experimental work by the percentage of glass fibers in weight per volume (kg per 1 m^3).

(a) (b)

Figure 1: (a) Glass fibers preparation, (b) glass fibers ready for use.

Table 1: C25 grade of concrete quantity per 1 m^3 by volume for mix of concrete.

Cement content	397 kg
Fine aggregate	682.9 kg
Course aggregate	1024.35 kg
Water/cement ratio	0.55
Glass fiber	0.25%, 0.50% and 0.75%

Using the above relative quantities of materials, forty-eight test beams of concrete are cast and cured for 7, 21, and 28 days and then tested at one point loading. Then the mix design proportion is used for the production of beams. First, gravel is spread in an even layer in the mixing pan mixer, followed by cement and sand, respectively. On top, a small amount of fiber is added to each ingredient. After 1 minute of dry mixing, water and the remaining fiber are added and the mixing operation continues for more than 3 minutes. Mixing of concrete should be done thoroughly to ensure that concrete of uniform quantity is obtained. Mixing is done using a machine mixer. Glass fiber consists of 200–400 individual filaments that are loosely linked together to form a stand. These stands can be chopped to different lengths or connected to create fabric mats or tape. It is impossible to mix more than 2% by volume of fibers with a length of 25 mm using traditional mixing techniques for normal concrete. Glass fiber has mostly been employed to reinforce the cement or mortar matrices used in the manufacture of thin-sheet products. In the case of reinforced plastics and AR-glass, E-glass has insufficient resistance to alkalis found in Portland cement, but AR-glass has better alkali-resistant properties. Polymers are sometimes added to the mixtures to improve physical qualities like moisture mobility.

2.3. Mixing, Casting, and Curing. The beams are cast in two sets. Set I consists of plain concrete with glass fiber at the end of 7 days, 21 days, and 28 days, and Set II is beam strength with both glass fiber and reinforcement bars at the end of 28 days. Set I consists of thirty-six beams in three series. Each series contains twelve plan concrete beams, three of which are control specimens, and the others are strengthened with GFRP, using 0.25%, 0.50%, and 0.75% at the end of 7, 21, and 28 days. Set II: twelve beam composite with GFRP and reinforced bars containing 0.25%, 0.50%, and 0.75%. All beams have a width of 150 mm, a total depth of 150 mm, and a total length of 750 mm. Compressive strength is studied for three samples for each of various proportional additions of fibers. Concrete compressive strength is typically determined by testing concrete cube molds with dimensions of 150 mm × 150 mm × 150 mm. The formwork with the steel cages is poured with concrete and compacted with a side vibrator at a uniform speed while the concrete is cast. After casting, the specimens are put in a water tank in the laboratory. The specimens are demolded after 1 day and a standard curing is done for 28 days after the casting of the specimens, and the whole process is shown in Figure 2 A-I.

2.4. Test for Compressive Strength of Concrete. The concrete mix is prepared with the calculated amount according to the mix design. Cubical molds are prepared and oiled properly in order to easily remove the concrete cubes from the mold. Concrete is filled in the cubical molds, and it is vibrated with an electric table vibrator so as to remove the air bubbles. The surface is smoothed and excess concrete is removed using a spatula, and the casting date is written on it. The mold is removed after 24 hours and the piece is placed in water for curing. The concrete specimens are tested for 28 days. The concrete specimens are loaded to failure using a concrete compressive strength testing machine, and the failure load is recorded. The stress is calculated by dividing the load at failure by the contact area of the specimen (the testing machine displayed the failure load and it also calculated the stress).

2.5. Flexural Testing Procedures for Experimental Tests and Setups. The RC beams are loaded under a center-point bending test with a 450 mm distance between supports. The flexural strength of specimens produced and cured in accordance with ASTM C293, "Standard Test Technique for Flexural Strength of Concrete Using Simple Beam with Center-Point Loading, is determined using this test method (ASTM C293). The beams are tested at one point of loading. At the center of the beam, this load reaches its maximum

Figure 2: (a) Wooden formwork ready for casting, (b) wooden formwork with the steel cage, (c) mixing of concrete and compaction of beam samples, (d) compacting and placing of concrete in the mold, (e) keeping in water tank, (f) reinforced set of beam, (g) cubical molds, (h) cube sample, (i) compressive strength test.

moment and deflection. The testing equipment is a Jack with a capacity of 2000 kN. The load is applied with a hydraulic Jack linked to an electric pump and measured with a computerized load cell. All the forty-eight beams are tested one by one: 36 plain concrete beams are strengthened only with glass fiber, 12 beams are strengthened both with GFRP and reinforced bars, and three control beams. The load on the beam elements is gradually increased until they reach their maximum capacity. Figure 3(a) shows a photograph of the test setup. The mid-span deflection and failure load for each beam are recorded. The flexural test setup consists of a microprocessor controlled (UTM) universal testing machine, as shown in Figure 4(b). The test setup is described in general compliance with the manufacturer's instructions. The UTM machine comprises two major components: the machine frame and the control. In our study, we used force control to apply the load in that force acts as an independent variable and displacement acts as a dependent variable.

In the study, we used three strain gage measurement on beam. Because single strain gauges can only successfully measure strain in one direction, using multiple strain gauges allows for more measurements to be obtained, resulting in a more precise assessment of strain on the surface being measured. To validate our result, we used [2] that studied on composites produced from chopped strand mat, and woven roving E-glass fiber were studied for their characteristics. Chopped strand mat composites outperformed woven roving E-glass fiber composites in terms of mechanical characteristics. The flexural test setup consists of a microprocessor controlled (UTM) universal testing machine with model UTM 70-C0807/C–C0820/C as shown in Figure 4(b). The general description of the test setup is in accordance with the manufacturer's instructions.

3. Results and Discussion

3.1. Compressive Strength of Concrete Test Results of Cube Samples (N/mm^2). Table 2 and Figure 5 show the 28 days compressive strength of concrete with maximum nominal size of aggregates 20 mm, by taking the average of the values overall an increase in the compressive strength is observed with the addition of fibers.

3.2. Flexural Test Results of Beam Samples. The different strength behaviors and characters, the crack pattern, and the failure modes of the tested beams throughout the experiment are presented in . The load on the beam elements is gradually increased until they achieve their maximum load carrying capacity as shown in Tables 3–6 and Figures 5–10.

3.3. Discussions of Test Results

3.3.1. Beams in Set II. In the control beams, the first beam failed at a maximum load of 83 kN with the formation of a diagonal crack at mid span in one side only, the second beam failed at an ultimate load of 89.8 kN by developing a diagonal crack at mid span in both sides, and the third beam failed at an ultimate load of 84.5 kN by developing a diagonal crack at mid span in one sides and the average ultimate load 85.76 kN and flexural strengthen 17.15 MPa. The appearance of a crack is first noted at average load 85.76 kN. As the load is increased, shear cracks increased in number, width, and depth. When the load is increased further, flexural failure in tension is the shear failure. The

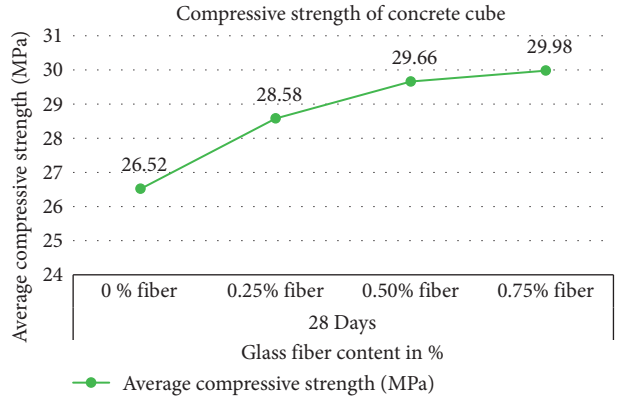

Figure 3: Effect of glass fibers on 28 day compressive strength.

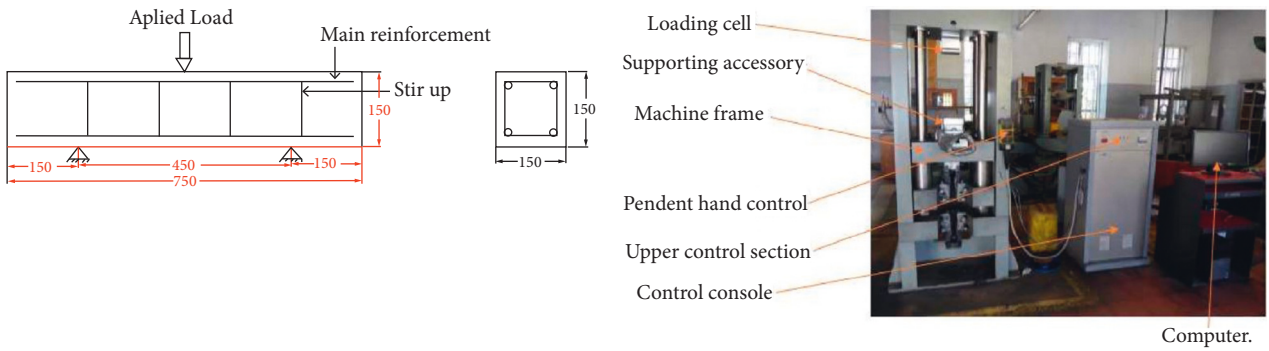

Figure 4: (a) Loading experimental setup, (b) test setup for concrete sample test under universal testing machine.

Table 2: Compressive strength of concrete cube.

Date	Glass fiber content (%)	Average compressive strength (N/mm^2)
28 days	0% fiber	26.52
	0.25% fiber	28.58
	0.50% fiber	29.66
	0.75% fiber	29.98

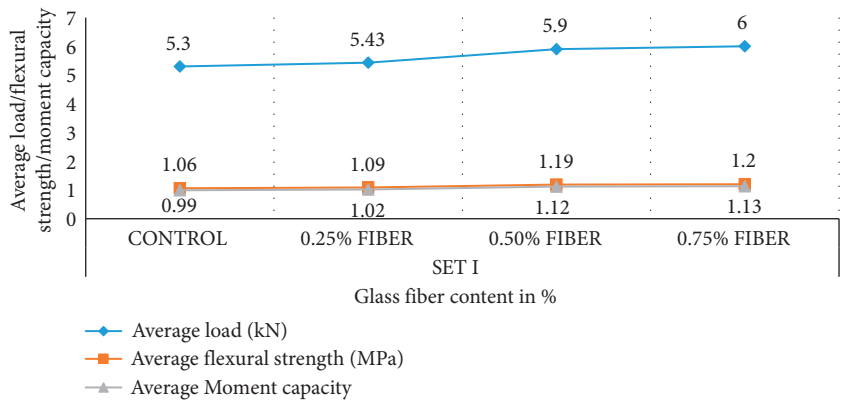

Figure 5: Average load/flexural strength/moment capacity versus glass fiber content on 7th day.

Table 3: Flexural strength of concrete 7 days test plain concrete beam samples.

Series	Sample spacemen	Average load (kN)	Average flexural strength (MPa)	Average moment capacity
Set I	Control	5.3	1.06	0.99
	0.25% fiber	5.43	1.09	1.02
	0.50% fiber	5.9	1.19	1.12
	0.75% fiber	6	1.2	1.13

Table 4: Flexural strength of concrete 21 days test plain concrete beam samples.

Series	Sample spacemen	Average load (kN)	Average flexural strength (MPa)	Average moment capacity
Set I	Control	16.8	3.36	3.15
	0.25% fiber	17	3.4	3.19
	0.50% fiber	17.2	3.44	3.23
	0.75% fiber	18.47	3.69	3.46

Table 5: Flexural strength of concrete 28 days test plain concrete beam samples.

Series	Sample spacemen	Average load (kN)	Average flexural strength (MPa)	Average moment capacity
Set I	Control	23.87	4.77	4.48
	0.25% fiber	24	4.8	4.5
	0.50% fiber	24.32	4.86	4.56
	0.75% fiber	24.45	4.89	4.58

Table 6: Average failure load, moment, and flexural strength of concrete beam samples after 28-days reinforced with glass fiber and reinforced bar.

Series	Sample spacemen	Average load (kN)	Average flexural strength (MPa)	Average Moment capacity
Set II	Control	85.76	17.15	16.08
	0.25% fiber	94.33	18.87	17.68
	0.50% fiber	103.33	20.67	19.37
	0.75% fiber	104.13	20.83	19.52

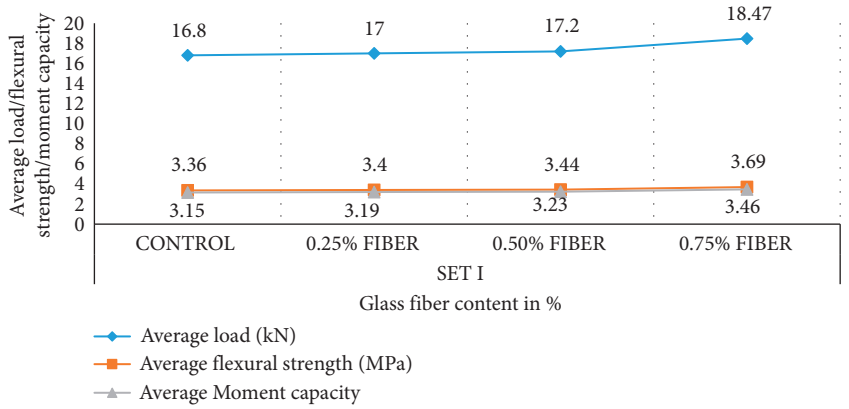

Figure 6: Average load/flexural strength/moment capacity versus glass fiber content on 21st day.

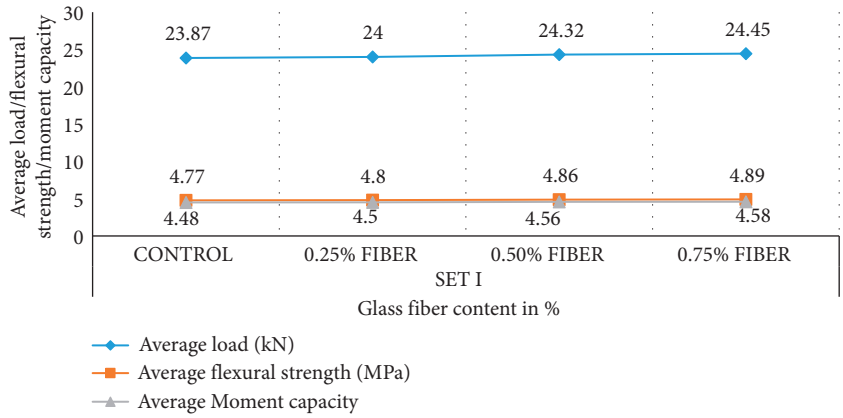

Figure 7: Average load/flexural strength/moment capacity versus glass fiber content on 28th day.

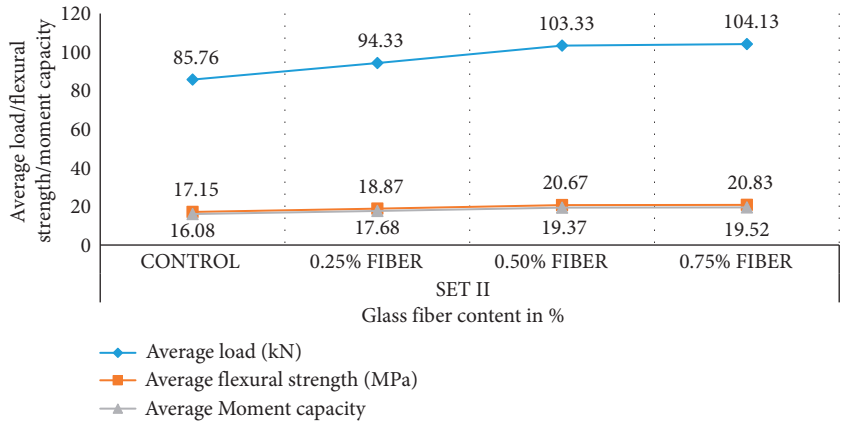

Figure 8: Average failure load, moment, and flexural strength of concrete beam samples after 28 days reinforced with glass fiber and reinforced bar.

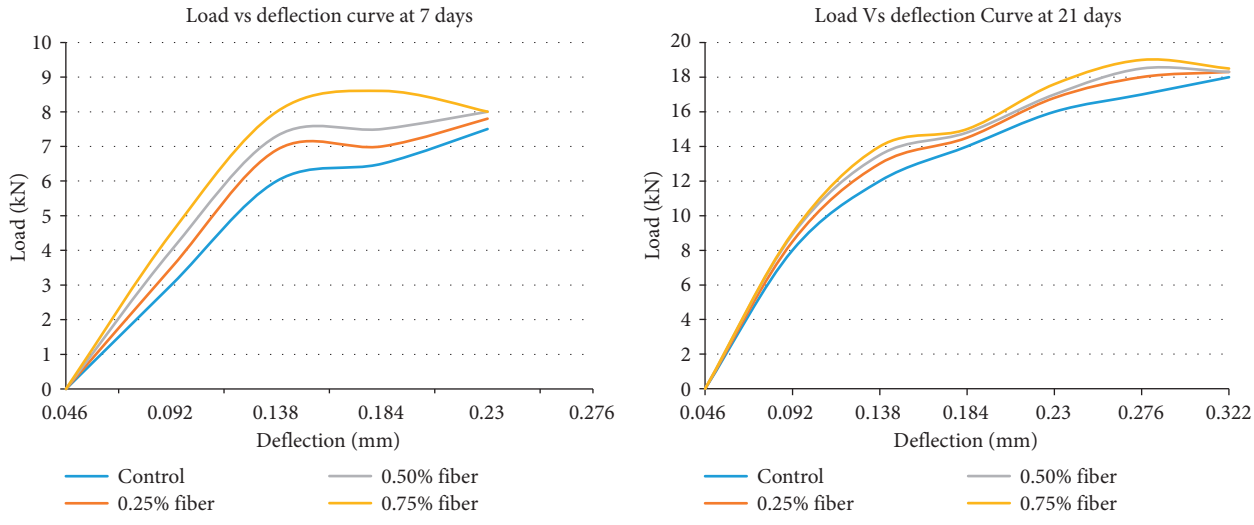

Figure 9: Continued.

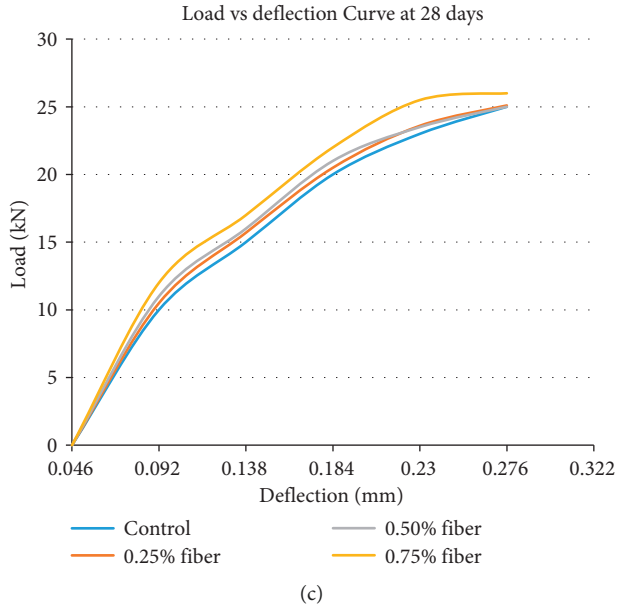

(c)

Figure 9: (a) Average load verses deflection comparison of set I beams at 7 days, (b) average load verses deflection comparison of set I beams at 21 days, average load verses deflection comparison of set I beams at 28 days.

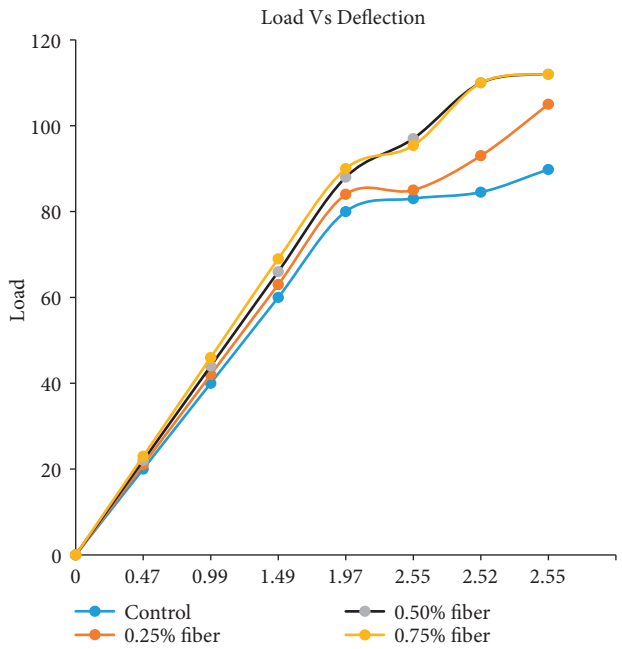

Figure 10: Comparison between load-deflection curves for control beam and strengthening beams for set II.

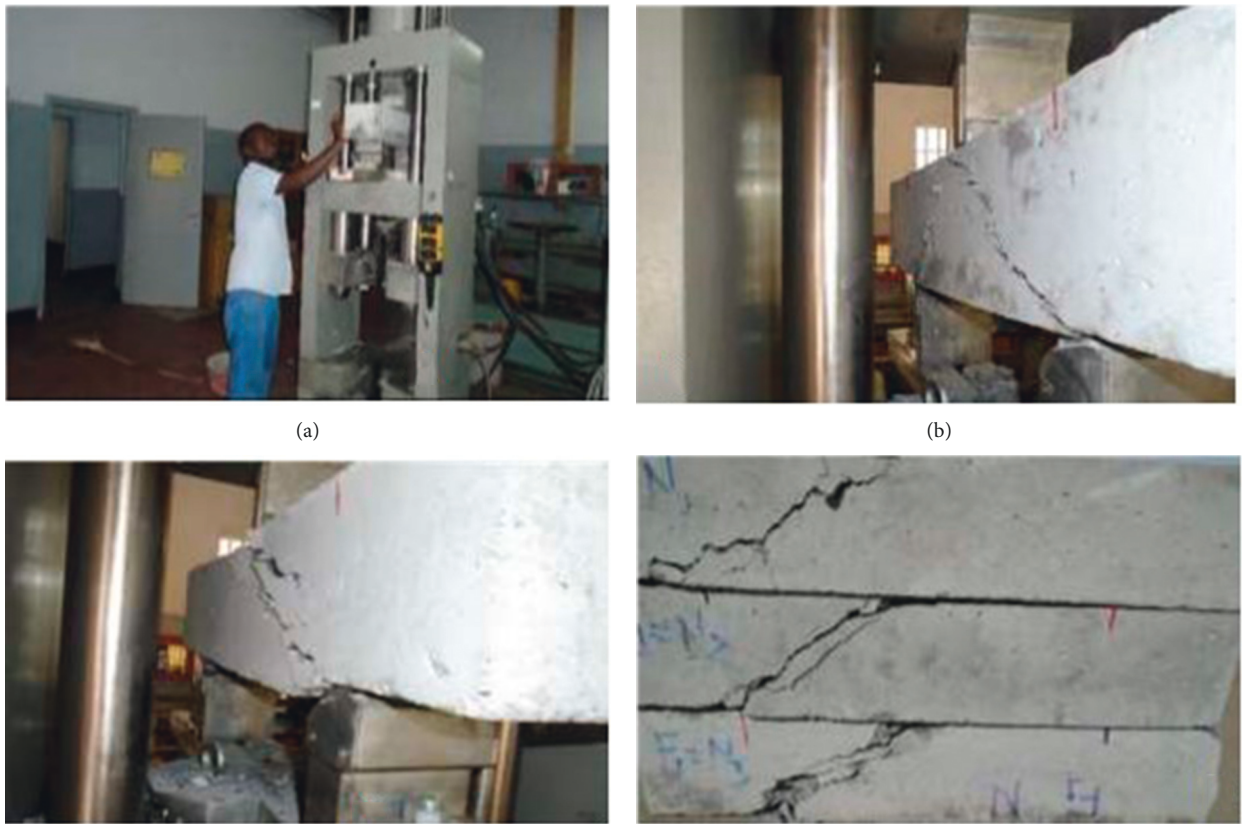

(a) (b)

(c) (d)

Figure 11: (a) Photos of failure of control beams, loading and marking, (b) photos of failure of control beams, testing, (c) photos of failure of control beams, starting of failure, (d) photos of failure of control beams, failure photo.

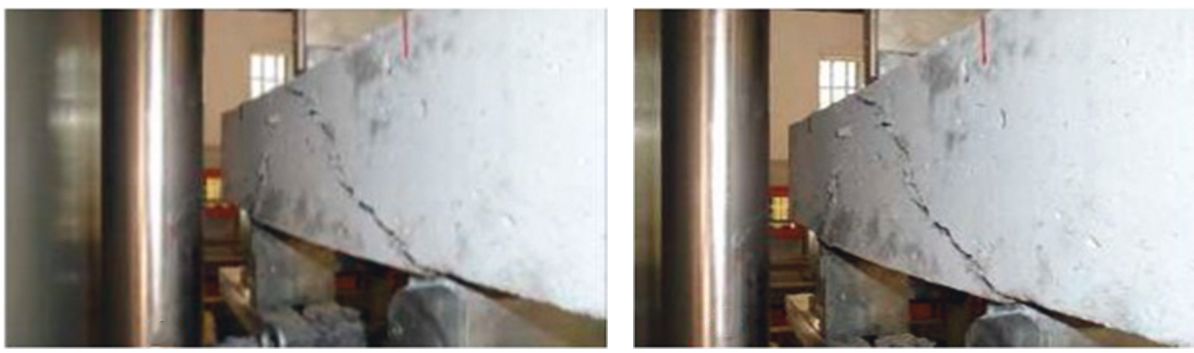

(a) (b)

Figure 12: Continued.

(c) (d)

Figure 12: (a) Photos of failure mode of tested beams with reinforced bar, control beam, (b) photos of failure mode of tested beams with reinforced bar, at 0.25% strength beam, (c) photos of failure mode of tested beams with reinforced bar, at 0.50% strength beam, (d) photos of failure mode of tested beams with reinforced bar, at 0.75% strength beam.

maximum deflection at failure is 7.75 mm as indicated in Figure 11.

3.4. Strengthening Beams. Beam strengthen with 0.25% fiber, the average ultimate load 94.33 kN, and flexural strengthen 18.87 MPa. Beam strengthen with 0.50% fiber, the average ultimate load of 103.33 kN, and flexural strength of 20.67 MPa. Beam strengthen with 0.75% fiber, the average ultimate load 104.13 kN, and flexural strengthen 20.83 MPa (Figure 12).

4. Conclusion

The experimental investigation of adding glass fibers to the concrete mix reached the following conclusions.

(i) The FRP material can be used for structural use, rather to its fabricated purpose of plaster reinforcement. The material is capable of increasing flexural capacity.

(ii) When compared to the control beam, all of the strengthen beams have a larger ultimate load-carrying capacity.

(iii) When compared to ordinary concrete, fiber-reinforced concrete provides higher strength. The following quantity of fiber 0.25%, 0.50%, and 0.75% is added in concrete, and their strength is compared with normal mix concrete and hence found that the concrete with glass fiber is stronger than normal mix.

(iv) The use of fibers considerably improved the flexural strength of concrete, and fiber-reinforced concrete has the potential to hold on to concrete cracks and prevent concrete beams from collapsing.

(v) When compared to the control beam, the enhanced beams fail at a higher load. Flexural strength of plain concrete beam shows tremendous increases from 2.5% to 13.2% at the end of 7 days, from 1.19% to 9.94% at the end of 21 days, from 0.54% to 2.45% at the end of 28 days are compared to control beams.

Generally, flexural strength-reinforced beams show tremendous increases from 2.91 to 13.60% compared to control beams. Observing at the flexural strength test result, the addition of glass fiber increased the flexural strength when compared with the control beams that is in line with [2].

Data Availability

All the data are available from the corresponding author upon request.

Conflicts of Interest

There are no conflicts of interest declared by the authors.

Acknowledgments

The authors wish to specially acknowledge Dr. Muftha Ahmed, faculty of civil engineering, Arba Minch University, Ethiopia, for his support and guidance. Getnet Melesse was supported by Arba Minch University (AMU/17/020135) for conducting the study.

References

[1] V. A. Kytinou, "Effect of steel fibers on the hysteretic performance of concrete beams with steel reinforcement—tests and analysis," *Materials*, vol. 13, 2020.

[2] V. V. Bhaskar, "Mechanical characterization of glass fiber (woven roving/chopped strand mat E-glass fiber) reinforced polyester composites," in *Proceedings of the AIP Conference Proceedings*, vol. 1859, AIP Publishing LLC, Article ID 020108, 2017.

[3] M. Serna Moreno, J. Martinez Vicente, and J. Lopez Cela, "Failure strain and stress fields of a chopped glass-reinforced polyester under biaxial loading," *Composite Structures*, vol. 103, pp. 27–33, 2013.

[4] F. Irine, "Strength aspects of basalt fiber reinforced concrete," *International Journal of Innovative Research in Advanced Engineering*, vol. 1, no. 8, pp. 192–198, 2014.

[5] W. A. Li, C. Ji, H. Zhu, F. Xing, J. Wu, and X. Niu, "Experimental investigation on the durability of glass fiber-reinforced polymer composites containing nanocomposite," *Journal of Nanomaterials*, vol. 2013, Article ID 352639, 11 pages, 2013.

[6] C. E. Chalioris and C. G. Karayannis, "Effectiveness of the use of steel fibres on the torsional behaviour of flanged concrete beams," *Cement and Concrete Composites*, vol. 31, no. 5, pp. 331–341, 2009.

[7] S. A. Dolati, A. Fereidoon, and A. R. Sabet, "Experimental investigation into glass fiber/epoxy composite laminates subjected to single and repeated high-velocity impacts of ice," *Iranian Polymer Journal (English Edition)*, vol. 23, no. 6, pp. 477–486, 2014.

[8] K. Y. Tshai, A. B. Chai, I. Kong, M. E. Hoque, and K. H. Tshai, "Hybrid fibre polylactide acid composite with empty fruit bunch: chopped glass strands," *Journal of Composites*, vol. 2014, Article ID 987956, 7 pages, 2014.

[9] H. A. Kaske Kassa, *A Study on Using Glass Fiber Reinforced Polymer Composites for Flexural Enhancement of Reinforced Concrete Beams*Heliyon, 2021.

[10] R. A. Jain, *Fiber Reinforced Polymer (FRP) Composites for Infrastructure Applications: Focusing on Innovation, Technology Implementation and Sustainability*, Springer Science & Business Media, Berlin, Germany, 2012.

[11] C. E.-M. Chalioris, "Cyclic response of steel fiber reinforced concrete slender beams: an experimental study," *Materials*, vol. 12, 2019.

[12] E. Bantie, *A study of flexural and compressive strengths of jute fibre-reinforced concrete*, Doctoral dissertation, PhD thesis, Addis Ababa University, Addis Ababa, Ethiopia, 2010.

[13] C. G. Karayannis, "Analysis and experimental study for steel fibre pullout from cementitious matrices," *Advanced Composites Letters*, vol. 9, no. 4, Article ID 096369350000900, 2000.

[14] M. A. Naghsh, A. Shishegaran, B. Karami et al., "An innovative model for predicting the displacement and rotation of column-tree moment connection under fire," *Frontiers of Structural and Civil Engineering*, vol. 15, no. 1, pp. 194–212, 2021.

[15] A. A. Shishegaran, M. R. Khalili, B. Karami, T. Rabczuk, and A. Shishegaran, "Computational predictions for estimating the maximum deflection of reinforced concrete panels subjected to the blast load," *International Journal of Impact Engineering*, vol. 139, Article ID 103527, 2020.